

Implicit-explicit, realizability-preserving first-order scheme for moment models with Lipschitz-continuous source terms

Florian Schneider^a

^a*Fachbereich Mathematik, TU Kaiserslautern, Erwin-Schrödinger-Str., 67663 Kaiserslautern, Germany,
schneider@mathematik.uni-kl.de*

Abstract

We derive an implicit-explicit (IMEX), realizability-preserving first-order scheme for moment models with Lipschitz-continuous source terms. In contrast to the fully-explicit schemes in [3, 42] the time step does not depend on the physical parameters, removing the stiffness from the system. Furthermore, a wider class of collision operators (e.g. the Laplace-Beltrami operator) can be used. The derived scheme is applied to minimum-entropy models.

Keywords: moment models, minimum entropy, implicit-explicit, realizability preservation

2010 MSC: 35L40, 35Q84, 65M08, 65M70, 65M60

1. Introduction

In recent years many approaches have been considered for the solution of time-dependent linear kinetic transport equations, which arise for example in electron radiation therapy or radiative heat transfer problems. Many of the most popular methods are moment methods, also known as moment closures because they are distinguished by how they close the truncated system of exact moment equations. Moments are defined through angular averages against basis functions to produce spectral approximations in the angle variable. A typical family of moment models are the so-called P_N -methods [16, 30] which are pure spectral methods. However, many high-order moment methods, including P_N , do not take into account that the original kinetic density to be approximated must be non-negative. The moment vectors produced by such models are therefore often not realizable, that is, there is no associated non-negative kinetic distribution consistent with the moment vector, and thus the solutions can contain non-physical artefacts such as negative local particle densities [5].

The family of minimum-entropy models, colloquially known as M_N models or entropy-based moment closures, solve this problem (for certain physically relevant entropies) by specifying the closure using a non-negative density reconstructed from the moments. The M_N models are the only models which additionally are hyperbolic and dissipate entropy [27]. The cost of all these properties is that the reconstruction of this density involves solving an optimization problem at every point on the space-time mesh [1, 2]. These reconstructions, however, can be parallelized, and so the recent emphasis on algorithms that can take advantage of massively parallel computing environments has led to renewed interest in the computation of M_N solutions both for linear and nonlinear kinetic equations [2, 9, 15, 18, 24, 31].

The key challenge for a numerical scheme is that, if not treated correctly, the numerical solution can leave the set of realizable moments [32], outside of which the defining optimization problem has no solution.

Discontinuous-Galerkin methods can handle this problem using a realizability limiter directly on the moment vectors themselves [3, 32, 47]. At this level realizability conditions are in general quite complicated and also

not well-understood for two- or three-dimensional problems for moment models of order higher than two. Realizability limiting for kinetic schemes [18, 42], however, is much easier because at the level of the kinetic density, realizability corresponds simply to non-negativity.

One big drawback of explicit schemes is that the time step depends on the physical parameters (absorption and scattering properties of the material), resulting in stiff systems, which can be avoided using an implicit discretization. On the other hand, the hyperbolic flux, which is non-linear and usually expensive to calculate, is typically non-stiff. An implicit discretization is therefore undesired. To overcome this we derive a realizability-preserving, first-order kinetic scheme with implicit-explicit (IMEX) time stepping, treating stiff and non-stiff problems separately.

The paper is organized as follows. A brief overview of the method of moment, the minimum-entropy approach and realizability is given in Section 2. Then, the reduced (space-homogeneous) moment system (which will be treated implicitly in the scheme) is investigated and the realizability-preserving property of this implicit discretization is shown in Section 3. This is concluded by the description of the full scheme and the proof that it is realizability-preserving in Section 4. The scheme is then tested in a manufactured solution and a benchmark test in Section 5. Finally, conclusions and an outlook on future work is given in Section 6.

2. Models

In slab geometry, the transport equation under consideration has the form

$$\partial_t \psi + \mu \partial_x \psi + \sigma_a \psi = \sigma_s \mathcal{C}(\psi) + Q, \quad t \in T, x \in X, \mu \in [-1, 1]. \quad (2.1)$$

The physical parameters are the absorption and scattering coefficient $\sigma_a, \sigma_s : T \times X \rightarrow \mathbb{R}_{\geq 0}$, respectively, and the emitting source $Q : T \times X \times [-1, 1] \rightarrow \mathbb{R}_{\geq 0}$. Furthermore, $\mu \in [-1, 1]$, and $\psi = \psi(t, x, \mu)$.

Assumption 2.1. *The operator \mathcal{C} is assumed to have the following properties.*

1. *Mass conservation*

$$\int_{-1}^1 \mathcal{C}(\psi) \, d\mu = 0. \quad (2.2a)$$

2. *Local entropy dissipation*

$$\int_{-1}^1 \eta'(\psi) \mathcal{C}(\psi) \, d\mu \leq 0, \quad (2.2b)$$

where η denotes a strictly convex entropy (compare Section 2.2).

3. *The reduced (space-homogeneous) system*

$$\partial_t \psi = \mathcal{C}(\psi), \quad (2.2c)$$

admits a non-negative solution $\psi \geq 0$ for all $t \geq 0$ and initial conditions $\psi(0, \mu) \geq 0$.

4. *For every $\Delta t \geq 0$, the following implication holds*

$$\psi(t, \mu) - \Delta t \mathcal{C}(\psi(t, \mu)) \geq 0 \Rightarrow \psi(t, \mu) \geq 0 \quad \text{for all } t \geq 0, \mu \in [-1, 1]. \quad (2.2d)$$

The first two assumptions are from [26], requiring that the operator is physically meaningful. The other assumptions are necessary for some of our proofs in the following¹. One example for such a collision operator is given by the Laplace-Beltrami operator

$$\mathcal{C}(\psi) = \frac{1}{2} \Delta_\mu \psi = \frac{1}{2} \frac{d}{d\mu} \left((1 - \mu^2) \frac{d\psi}{d\mu} \right). \quad (2.3)$$

This operator appears, for example, as the result of an asymptotic analysis of the Boltzmann equation under the assumption of small energy loss and deflection, and forward-peaked scattering in the context of electron transport [14, 19, 34].

Another typical choice is the linear integral collision operator

$$\mathcal{C}(\psi) = \int_{-1}^1 K(\mu, \mu') \psi(t, \mathbf{x}, \mu') d\mu' - \int_{-1}^1 K(\mu', \mu) \psi(t, \mathbf{x}, \mu) d\mu'. \quad (2.4)$$

The collision kernel K is assumed to be strictly positive, symmetric (i.e. $K(\mu, \mu') = K(\mu', \mu)$) and normalized to $\int_{-1}^1 K(\mu', \mu) d\mu' = 1$. A typical example is the BGK-type *isotropic-scattering* operator, where $K(\mu, \mu') \equiv \frac{1}{2}$.

The transport equation (2.1) is supplemented by initial and boundary conditions:

$$\psi(0, x, \mu) = \psi_{t=0}(x, \mu) \quad \text{for } x \in X = (x_L, x_R), \mu \in [-1, 1], \quad (2.5a)$$

$$\psi(t, x_L, \mu) = \psi_b(t, x_L, \mu) \quad \text{for } t \in T, \mu > 0, \quad (2.5b)$$

$$\psi(t, x_R, \mu) = \psi_b(t, x_R, \mu) \quad \text{for } t \in T, \mu < 0. \quad (2.5c)$$

2.1. The method of moments

In general, solving equation (2.1) is very expensive in two and three dimensions due to the high dimensionality of the state space.

For this reason it is convenient to use some type of spectral or Galerkin method to transform the high-dimensional equation into a system of lower-dimensional equations. Typically, one chooses to reduce the dimensionality by representing the angular dependence of ψ in terms of some basis \mathbf{b} .

Definition 2.2. *The vector of functions $\mathbf{b} : [-1, 1] \rightarrow \mathbb{R}^n$ consisting of n basis functions b_i , $i = 0, \dots, n-1$ of maximal order N is called an angular basis. Analogously, the symbol \mathbf{b}_N can be used if the knowledge of N is explicitly necessary.*

The so-called moments of a given distribution function ψ with respect to \mathbf{b} are then defined by

$$\mathbf{u} = \langle \mathbf{b} \psi \rangle = (u_0, \dots, u_{n-1})^T, \quad (2.6)$$

where the integration $\langle \cdot \rangle = \int_{-1}^1 \cdot d\mu$ is performed componentwise.

Assuming for simplicity $b_0 \equiv 1$, the quantity $u_0 = \langle b_0 \psi \rangle = \langle \psi \rangle$ is called local particle density. Furthermore, normalized moments $\boldsymbol{\phi} = (\phi_1, \dots, \phi_{n-1}) \in \mathbb{R}^n$ are defined as

$$\phi_i = \frac{u_i}{u_0}, \quad i = 1, \dots, n-1. \quad (2.7)$$

¹To be completely correct, the assumptions have to be formulated in a weak sense. However, all steps below can be performed similarly but with a greater notational effort.

To obtain a set of equations for \mathbf{u} , (2.1) has to be multiplied through by \mathbf{b} and integrated over $[-1, 1]$, giving

$$\langle \mathbf{b} \partial_t \psi \rangle + \langle \mathbf{b} \partial_x \mu \psi \rangle + \langle \mathbf{b} \sigma_a \psi \rangle = \sigma_s \langle \mathbf{b} \mathcal{C}(\psi) \rangle + \langle \mathbf{b} Q \rangle.$$

Collecting known terms, and interchanging integrals and differentiation where possible, the moment system has the form

$$\partial_t \mathbf{u} + \partial_x \langle \mu \mathbf{b} \hat{\psi}_{\mathbf{u}} \rangle + \sigma_a \mathbf{u} = \sigma_s \langle \mathbf{b} \mathcal{C}(\hat{\psi}_{\mathbf{u}}) \rangle + \langle \mathbf{b} Q \rangle. \quad (2.8)$$

The solution of (2.8) is equivalent to the one of (2.1) if \mathbf{b} is a basis of $L_2([-1, 1], \mathbb{R})$.

Since it is impractical to work with an infinite-dimensional system, only a finite number of $n < \infty$ basis functions \mathbf{b} of order N can be considered. Unfortunately, there always exists an index $i \in \{0, \dots, n-1\}$ such that the components of $b_i \cdot \mu$ are not in the linear span of \mathbf{b} . Therefore, the flux term cannot be expressed in terms of \mathbf{u} without additional information. Furthermore, the same might be true for the projection of the scattering operator onto the moment-space given by $\langle \mathbf{b} \mathcal{C}(\psi) \rangle$. This is the so-called *closure problem*. One usually prescribes some *ansatz* distribution $\hat{\psi}_{\mathbf{u}}(t, \mathbf{x}, \mu) := \hat{\psi}(\mathbf{u}(t, \mathbf{x}), \mathbf{b}(\mu))$ to calculate the unknown quantities in (2.8). Note that the dependence on the angular basis in the short-hand notation $\hat{\psi}_{\mathbf{u}}$ is neglected for notational simplicity.

Finally, we write (2.8) in the form of a standard first-order hyperbolic system of equations:

$$\partial_t \mathbf{u} + \partial_x \mathbf{F}(\mathbf{u}) = \mathbf{s}(\mathbf{u}), \quad (2.9)$$

where $\mathbf{F}(\mathbf{u}) = \langle \mu \mathbf{b} \hat{\psi}_{\mathbf{u}} \rangle$ and $\mathbf{s}(\mathbf{u}) = \sigma_s \langle \mathbf{b} \mathcal{C}(\hat{\psi}_{\mathbf{u}}) \rangle + \langle \mathbf{b} Q \rangle - \sigma_a \mathbf{u}$.

2.2. Minimum-entropy approach

In this paper the ansatz density $\hat{\psi}$ is reconstructed from the moments \mathbf{u} by minimizing the entropy-functional

$$\mathcal{H}(\psi) = \langle \eta(\psi) \rangle \quad (2.10)$$

under the moment constraints

$$\langle \mathbf{b} \psi \rangle = \mathbf{u}. \quad (2.11)$$

The kinetic entropy density $\eta : \mathbb{R} \rightarrow \mathbb{R}$ is strictly convex and twice continuously differentiable and the minimum is simply taken over all functions $\psi = \psi(\mu)$ such that $\mathcal{H}(\psi)$ is well defined. The obtained ansatz $\hat{\psi} = \hat{\psi}_{\mathbf{u}}$, solving this constrained optimization problem, is given by

$$\hat{\psi}_{\mathbf{u}} = \underset{\psi : \langle \eta(\psi) \rangle < \infty}{\operatorname{argmin}} \{ \langle \eta(\psi) \rangle : \langle \mathbf{b} \psi \rangle = \mathbf{u} \}. \quad (2.12)$$

This problem, which must be solved over the space-time mesh, is typically solved through its strictly convex finite-dimensional dual,

$$\boldsymbol{\alpha}(\mathbf{u}) := \underset{\tilde{\boldsymbol{\alpha}} \in \mathbb{R}^n}{\operatorname{argmin}} \left\langle \eta_*(\mathbf{b}^T \tilde{\boldsymbol{\alpha}}) \right\rangle - \mathbf{u}^T \tilde{\boldsymbol{\alpha}}, \quad (2.13)$$

where η_* is the Legendre dual of η . The first-order necessary conditions for the multipliers $\boldsymbol{\alpha}(\mathbf{u})$ show that the solution to (2.12) has the form

$$\hat{\psi}_{\mathbf{u}} = \eta'_* \left(\mathbf{b}^T \boldsymbol{\alpha}(\mathbf{u}) \right) \quad (2.14)$$

where η'_* is the derivative of η_* .

This approach is called the *minimum-entropy closure* [26]. The resulting model has many desirable properties: symmetric hyperbolicity, bounded eigenvalues of the directional flux Jacobian and the direct existence of an entropy-entropy flux pair (compare [26, 40]).

The kinetic entropy density η can be chosen according to the physics being modelled. As in [18, 26], Maxwell-Boltzmann entropy

$$\eta(\psi) = \psi \log(\psi) - \psi \quad (2.15)$$

is used, thus $\eta_*(p) = \eta'_*(p) = \exp(p)$. This entropy is used for non-interacting particles as in an ideal gas.

We use the modification of the adaptive-basis optimization routine [1] as proposed in [42] to solve (2.13).

Substituting ψ in (2.8) with $\hat{\psi}_{\mathbf{u}}$ yields a closed system of equations for \mathbf{u} :

$$\partial_t \mathbf{u} + \partial_x \langle \mu \mathbf{b} \hat{\psi}_{\mathbf{u}} \rangle + \sigma_a \mathbf{u} = \sigma_s \langle \mathbf{b} \mathcal{C}(\hat{\psi}_{\mathbf{u}}) \rangle + \langle \mathbf{b} Q \rangle. \quad (2.16)$$

In this paper, the full-moment basis $\mathbf{b} = (1, \mu, \dots, \mu^N)$ will be used. Nevertheless, the scheme can be transferred directly to other bases like the *half-moment monomial basis* ($b_i = \mathbb{1}_{[-1,0]} \mu^i$ or $b_i = \mathbb{1}_{[0,1]} \mu^i$) [10, 11, 36] or the mixed-moment basis ($\mathbf{b} = (1, \mu \mathbb{1}_{[0,1]}, \dots, \mu^N \mathbb{1}_{[0,1]}, \mu \mathbb{1}_{[-1,0]}, \dots, \mu^N \mathbb{1}_{[-1,0]})$) [14, 41, 43]. Similarly, the results are not restricted to the minimum-entropy approach but can be transferred to other realizable closures like Kershaw [22, 38, 39] or the quadrature method of moments [12, 13, 45, 46].

2.3. Realizability

Since the underlying kinetic density to be approximated is non-negative, a moment vector only makes sense physically if it can be associated with a non-negative distribution function. In this case the moment vector is called *realizable*.

Definition 2.3. The realizable set $\mathcal{R}_{\mathbf{b}}$ is

$$\mathcal{R}_{\mathbf{b}} = \{ \mathbf{u} : \exists \psi(\mu) \geq 0, u_0 = \langle \psi \rangle > 0, \text{ such that } \mathbf{u} = \langle \mathbf{b} \psi \rangle \}.$$

If $\mathbf{u} \in \mathcal{R}_{\mathbf{b}}$, then \mathbf{u} is called *realizable*. Any ψ such that $\mathbf{u} = \langle \mathbf{b} \psi \rangle$ is called a *representing density*.

Remark 2.4.

- (a) The realizable set is a convex cone, and
- (b) Representing densities are not necessarily unique.

Additionally, since the entropy ansatz has the form (2.14), in the Maxwell-Boltzmann case, the optimization problem (2.12) only has a solution if the moment vector lies in the ansatz space

$$\mathcal{A} := \left\{ \langle \mathbf{b} \hat{\psi}_{\mathbf{u}} \rangle \stackrel{(2.14)}{=} \langle \mathbf{b} \eta'_* (\mathbf{b}^T \boldsymbol{\alpha}) \rangle : \boldsymbol{\alpha} \in \mathbb{R}^n \right\}.$$

In the case of a bounded angular domain, the ansatz space \mathcal{A} is equal to the set of realizable moment vectors [21]. Therefore, it is sufficient to focus on realizable moments only.

The definition of the realizable set is not constructive, making it hard to check if a moment vector is realizable or not. There are several works about concrete representations of the realizable set for different bases, e.g. [3, 6, 7, 22, 41, 43].

Exemplarily, the full-moment realizable set of order $N = 2$ is given by [7]

$$\mathcal{R}_{\mathbf{b}} = \{\mathbf{u} \in \mathbb{R}^3 : u_0 \geq |u_1|, u_0 u_2 \geq u_1^2\}. \quad (2.17)$$

Fortunately, since we only use a first-order scheme, no information about the realizable set (except its convexity) is needed in the following. Note that this might no longer be true when higher-order schemes (in space and time) are used, see e.g. [42, 47, 48].

3. Realizability of the reduced equation

Before treating the space-dependent transport equation (2.1), we want to investigate (2.2c) in more detail. The following example shows why explicit schemes for the Laplace-Beltrami fail.

Example 3.1.

$$\partial_t \mathbf{u} = \langle \mathbf{b} \Delta_\mu \hat{\psi}_{\mathbf{u}} \rangle, \quad (3.1)$$

where the ansatz $\hat{\psi}_{\mathbf{u}}$ can be chosen accordingly as (2.14), if necessary.

It is possible to show that (2.2c) has a solution in $L_2([-1, 1], \mathbb{R}_{\geq 0})$ for every $t \geq 0$ [17, 20, 23, 35]. Therefore, it is possible to expand ψ in μ in terms of the Legendre polynomials P_i , which form an orthogonal basis of L_2 and are eigenfunctions of Δ_μ . Then, (2.2c) transforms to

$$\sum_{i=0}^{\infty} (\partial_t \alpha_i + i(i+1) \alpha_i) c_i P_i = 0,$$

where the coefficients c_i are normalization constants. This equation can be stated equivalently as an infinite, decoupled system of ordinary differential equations

$$\partial_t \alpha_i = -i(i+1) \alpha_i, \quad i \in \mathbb{N}_{\geq 0}$$

with solution

$$\alpha_i(t) = e^{-i(i+1)t} \alpha_i(0),$$

where $\alpha_i(0)$ are the Fourier coefficients of $\psi(0, \mu)$. For $t \rightarrow \infty$ it obviously holds that

$$\lim_{t \rightarrow \infty} \alpha_i(t) = 0, \quad i = 1, \dots, \infty$$

which means that $\psi(t, \mu) \xrightarrow{t \rightarrow \infty} \alpha_0(0)$. This implies that for every initial condition for (2.2c) a stationary solution is attained and that it is isotropic. This is not very surprising since the constants are in the kernel of Δ_μ .

The corresponding second-order, full-moment vector field

$$\langle \mathbf{b}_2 \Delta_\Omega \hat{\psi} \rangle = (0, -2u_1, -6u_2 + 2u_0)^T \quad (3.2)$$

is plotted in normalized moments in Figure 1.

Some solution curves (red dotted), starting at the realizability boundary (red triangles), are shown as well. All those curves end in the isotropic point (red dot) implying that the stationary solution of (2.2c) is recovered. This is not by accident. The solution of (3.1) with a full-moment basis turns out to be just the

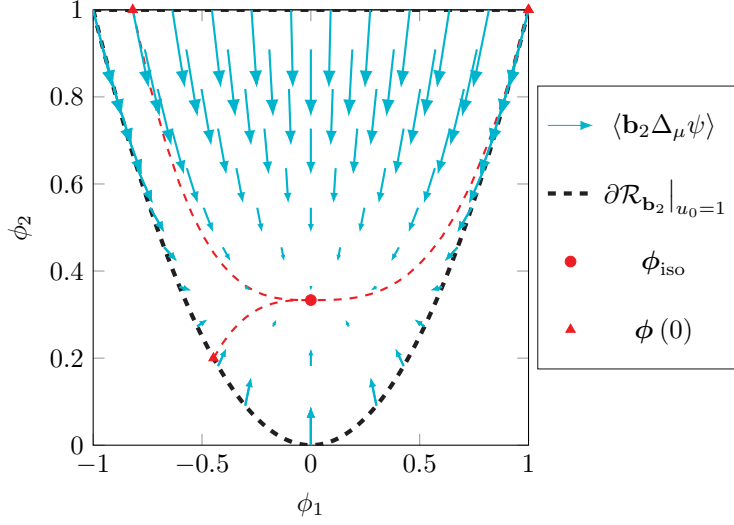


Figure 1: Vector field of the right-hand side and some solution trajectories of (3.2) for $N = 2$ and $u_0 = 1$. The length of the arrows is scaled by 0.03.

projection of (2.2c) onto the corresponding moment space. This is proven below in Lemma 3.4.

As visible in Figure 1, the vector field in $\pm\phi_1 = \phi_2 = 1$ is tangential to the realizability boundary $\partial\mathcal{R}_{\mathbf{b}_2}|_{u_0=1}$. Therefore, no explicit time discretization of (3.1) generally preserves realizability using a fixed non-negative time step.

This can be shown by a simple calculation. Due to (2.2a), it suffices to choose $u_0 = 1$ and therefore the explicit discretization with step size Δt in normalized moments reads

$$\begin{aligned}\phi_1(t + \Delta t) &= \phi_1(t) - 2\Delta t\phi_1(t), \\ \phi_2(t + \Delta t) &= \phi_2(t) - 6\Delta t\phi_2(t) + 2\Delta t.\end{aligned}$$

Plugging in $\phi(t) = (1, 1)$, the updated normalized moment is given by

$$\begin{aligned}\phi_1(t + \Delta t) &= 1 - 2\Delta t, \\ \phi_2(t + \Delta t) &= 1 - 4\Delta t.\end{aligned}$$

The update $\phi(t + \Delta t)$ is realizable (see (2.17)) if

$$1 \geq \phi_2(t + \Delta t) = 1 - 4\Delta t \geq \phi_1(t + \Delta t)^2 = (1 - 2\Delta t)^2 = 1 - 4\Delta t + 4\Delta t^2.$$

The last inequality implies $4\Delta t^2 \leq 0$, which is for $\Delta t \in \mathbb{R}$ only possible if $\Delta t = 0$.

Remark 3.2. This is in contrast to the linear collision operator (2.4), which is in principle easy to control since its moments are always of the form

$$\langle \mathbf{b}\mathcal{C}(\psi) \rangle = \tilde{\mathbf{u}} - \mathbf{u},$$

where $\tilde{\mathbf{u}} \in \mathcal{R}_{\mathbf{b}}$ [3]. Note that this is true for any angular basis, not only for full moments. Since the realizable set is a convex cone, this additional realizable term does not affect the realizability of the moment systems solution in a negative way, even if everything is discretized explicitly. The explicit update for (3.1) reads

$$\mathbf{u}(t + \Delta t) = (1 - \Delta t)\mathbf{u}(t) + \Delta t\tilde{\mathbf{u}},$$

which is realizable as long as $0 \leq \Delta t \leq 1$. This corresponds to the standard stability condition for the explicit Euler scheme and depends on the stiffness of the system under consideration.

As a consequence of Assumption 2.1(3), the solution ψ of (2.2c) is non-negative. Using this information one can conclude realizability of the exact solution of

$$\partial_t \mathbf{u} = \left\langle \mathbf{b} \mathbf{C} \left(\hat{\psi}_{\mathbf{u}} \right) \right\rangle =: \mathbf{C}(\mathbf{u}), \quad (3.3)$$

under the following assumptions.

Assumption 3.3. (a) The map $\mathbf{u} \rightarrow \left\langle \mathbf{b} \mathbf{C} \left(\hat{\psi}_{\mathbf{u}} \right) \right\rangle$ is Lipschitz-continuous in \mathbf{u} (with respect to any norm in \mathbb{R}^n)

(b) (3.3) admits a unique solution $\mathbf{u}(t)$ for all $t \geq 0$.

Lemma 3.4.

Let $\mathbf{u}(0) \in \mathcal{R}_{\mathbf{b}}$ and Assumption 3.3 be valid. Then, the solution $\mathbf{u}(t)$ of (3.3) satisfies $\mathbf{u}(t) \in \mathcal{R}_{\mathbf{b}}$ for all $t \geq 0$.

Proof. Let $\psi(t, \mu)$ denote the solution of (2.2c). As mentioned before, $\psi(t, \mu) \geq 0$ for all $t \geq 0$ and $\mu \in [-1, 1]$. Defining the moments of ψ as $\mathbf{u}_{\psi} = \langle \mathbf{b} \psi \rangle$, it is immediately obvious that \mathbf{u}_{ψ} also solves (3.3) and $\mathbf{u}_{\psi}(t) \in \mathcal{R}_{\mathbf{b}}$ for all $t \geq 0$. Due to the uniqueness of the solution of (3.3) (Assumption 3.3(b)) it follows that $\mathbf{u} = \mathbf{u}_{\psi}$, which completes the proof. \square

Consequently, an implicit discretization of the moment system preserves realizability.

Corollary 3.5. Let $\mathbf{u}(0) \in \mathcal{R}_{\mathbf{b}}$. Then the implicit time-discretization

$$\mathbf{u}(t + \Delta t) = \mathbf{u}(t) + \Delta t \mathbf{C}(\mathbf{u}(t + \Delta t)) \quad (3.4)$$

of (3.3) satisfies $\mathbf{u}(t) \in \mathcal{R}_{\mathbf{b}}$ for all $t = j\Delta t$, $j \in \mathbb{N}$.

Proof. Similar to the proof of Lemma 3.4, one can make use of the discretization of the kinetic equation (2.2c), which reads

$$\psi(t + \Delta t, \mu) = \psi(t, \mu) + \Delta t \mathbf{C}(\psi(t + \Delta t, \mu)).$$

Using (2.2d) it follows that $\psi(t + \Delta t, \mu) \geq 0$, since by assumption $\psi(t, \mu) \geq 0$.

The solution of the system (3.4) is unique by Banach's fixed point theorem (using a norm that is suitably scaled by the Lipschitz constant of \mathbf{C}). As above, this solution has to satisfy $\mathbf{u}(t + \Delta t) = \langle \mathbf{b} \psi(t + \Delta t) \rangle$ and is therefore realizable. \square

Example 3.6. We want to show that the Laplace-Beltrami operator satisfies (2.2d).

Assuming that at time t the solution is non-negative, the implicit discretization of (2.2c) can be written as

$$(I - \Delta t \Delta_{\mu}) \psi(t + \Delta t) = \psi(t) \geq 0. \quad (3.5)$$

Since the Laplace-Beltrami operator is a negative operator, the operator $(I - \Delta t \Delta_{\mu})$ is positive and consequently $\psi(t + \Delta t) \geq 0$. This can be derived rigorously by defining the Hilbert space

$$\mathcal{V} = \{v \in L_2(-1, 1) \mid \sqrt{1 - \mu^2} \frac{dv}{d\mu} \in L_2(-1, 1)\}$$

with the inner product

$$(v, \psi)_{\mathcal{V}} = \left\langle v\psi + \Delta t(1 - \mu^2) \frac{dv d\psi}{d\mu d\mu} \right\rangle$$

and the induced norm $\|v\|_{\mathcal{V}} = \sqrt{(v, v)_{\mathcal{V}}}$. These definitions roughly follow [8]. The weak formulation of (3.5) reads

$$(v, \psi(t + \Delta t))_{\mathcal{V}} = \langle v\psi(t) \rangle.$$

Choosing $v = \psi^-(t + \Delta t) = \min(0, \psi(t + \Delta t))$, the weak formulation turns to

$$\|\psi^-(t + \Delta t)\|_{\mathcal{V}}^2 = \left\langle \underbrace{\psi^-(t + \Delta t)}_{\leq 0} \underbrace{\psi(t)}_{\geq 0} \right\rangle \leq 0.$$

Therefore, $\psi^-(t + \Delta t) \equiv 0$ almost everywhere and consequently $\psi(t + \Delta t) \geq 0$ almost everywhere.

Remark 3.7. We want to remark that both collision operators (2.3) and (2.4) with the full-moment basis satisfy all the previous assumptions since in both cases the operator $\mathbf{C}(\mathbf{u})$ is linear in \mathbf{u} .

4. Realizability-preserving first-order scheme

It is easy to show that a standard explicit, first-order finite-volume scheme for (2.16) with suitably-chosen numerical fluxes automatically preserves the realizability of the underlying solution under a CFL-type constraint if the moments of the collision operator can be written as $\langle \mathbf{bC}(\psi) \rangle = \tilde{\mathbf{u}} - \mathbf{u}$, where $\tilde{\mathbf{u}} \in \mathcal{R}_{\mathbf{b}}$ is realizable (see e.g. [3, 18, 42]).

Unfortunately, this is in general not possible for the Laplace-Beltrami operator. As has been shown above, an explicit discretization of the right-hand-side of (2.16) can lead to unrealizable moments even in the rather simple case of the full-moment M_2 model. This results from the fact that the vector field defined by $\langle \mathbf{bC}(\psi) \rangle$ can point tangential to the realizability boundary and can be avoided using an implicit discretization.

On the other hand, the hyperbolic flux, which is non-linear and usually expensive to calculate, is typically non-stiff. An implicit discretization is therefore undesired.

To overcome this, we treat the two parts separately using an implicit-explicit time-stepping.

In the following, the spatial domain $X = (x_L, x_R)$ is divided into (for notational simplicity) n_x (equidistant) cells $I_j = (x_{j-\frac{1}{2}}, x_{j+\frac{1}{2}})$, where the cell interfaces are given by $x_{j\pm\frac{1}{2}} = x_j \pm \frac{\Delta x}{2}$ for cell centres $x_j = x_L + (j - \frac{1}{2})\Delta x$, and $\Delta x = \frac{x_R - x_L}{n_x}$.

Defining the averaging operator

$$\bar{\cdot}_j := \frac{1}{\Delta x} \int_{I_j} \cdot dx,$$

the discretized form of (2.9) reads

$$\frac{\bar{\mathbf{u}}_j^{(\kappa+1)} - \bar{\mathbf{u}}_j^{(\kappa)}}{\Delta t} = -\frac{1}{\Delta x} \left(\widehat{\mathbf{F}}(\bar{\mathbf{u}}_j^{(\kappa)}, \bar{\mathbf{u}}_{j+1}^{(\kappa)}) - \widehat{\mathbf{F}}(\bar{\mathbf{u}}_{j-1}^{(\kappa)}, \bar{\mathbf{u}}_j^{(\kappa)}) \right) + \mathbf{s}(\bar{\mathbf{u}}_j^{(\kappa+1)}) \quad (4.1)$$

where $\widehat{\mathbf{F}}$ is a numerical flux function coupling the solution on cell I_j with its neighbours.

We use the kinetic flux (see e.g. [15, 18, 42])

$$\widehat{\mathbf{F}}(\mathbf{u}_1, \mathbf{u}_2) = \langle \mathbf{b} h(\psi_1, \psi_2) \rangle, \quad \text{where} \quad (4.2)$$

$$h(\psi_1, \psi_2) = \begin{cases} \mu \psi_1 & \text{if } \mu \geq 0, \\ \mu \psi_2 & \text{if } \mu \leq 0 \end{cases} \quad (4.3)$$

and $\psi_{1,2}$ are the ansätze for $\mathbf{u}_{1,2}$, respectively. This is generally possible for minimum-entropy and Kershaw models by carrying out the integrations over the half-spaces separated by $\mu = 0$. This is particularly easy in case of half- and mixed-moment models since then the numerical flux can be explicitly written in terms of the moments instead of some half moments of the ansatz function.

The incorporation of boundary conditions is non-trivial. Here, an often-used approach is taken that incorporates boundary conditions via ‘ghost cells’. First assume that it is possible to smoothly extend $\psi_b(t, x, \mu)$ in μ to $[-1, 1]$ for $x \in \{x_L, x_R\}$ (note that while moments are defined using integrals over all μ , the boundary conditions in (2.5b)–(2.5c) are only defined for μ corresponding to incoming data).

Then the moment approximations in the ghost cells at x_0 and x_{n_x+1} simply take the form

$$\mathbf{u}_0(t, x_{\frac{1}{2}}) := \langle \mathbf{b} \psi_b(t, x_L, \mu) \rangle, \quad (4.4a)$$

$$\mathbf{u}_{n_x+1}(t, x_{n_x+\frac{1}{2}}) := \langle \mathbf{b} \psi_b(t, x_R, \mu) \rangle. \quad (4.4b)$$

Note, however, that the validity of this approach, due to its inconsistency with the original boundary conditions (2.5b)–(2.5c), is not entirely non-controversial, but the question of appropriate boundary conditions for moment models is an open problem [25, 29, 33, 37, 44] which is not explored here.

The IMEX time-stepping in (4.1) uses the forward-backward Euler scheme [4]. Since this is nothing else than doing a Godunov splitting of the hyperbolic part (treated explicitly) and the (stiff) source term (treated implicitly), the following theorem can be concluded.

Theorem 4.1. *Let $\bar{\mathbf{u}}_j^{(\kappa)} \in \mathcal{R}_{\mathbf{b}}$ for all $j = 0, \dots, n_x+1$. Furthermore, let Assumption 2.1 and Assumption 3.3 hold, and $\sigma_a(t, x), \sigma_s(t, x), Q(t, x, \mu) \in \mathbb{R}_{\geq 0}$ be bounded and continuous in t .*

Then, the IMEX scheme (4.1) preserves realizability (i.e. $\bar{\mathbf{u}}_j^{(\kappa+1)} \in \mathcal{R}_{\mathbf{b}}$ for all $j = 1, \dots, n_x$) under the CFL condition

$$\Delta t \leq \Delta x. \quad (4.5)$$

Proof. The scheme (4.1) is equivalent to the following splitting scheme

$$\bar{\mathbf{u}}_j^{(*)} = \bar{\mathbf{u}}_j^{(\kappa)} - \frac{\Delta t}{\Delta x} \left(\widehat{\mathbf{F}}(\bar{\mathbf{u}}_j^{(\kappa)}, \bar{\mathbf{u}}_{j+1}^{(\kappa)}) - \widehat{\mathbf{F}}(\bar{\mathbf{u}}_{j-1}^{(\kappa)}, \bar{\mathbf{u}}_j^{(\kappa)}) \right), \quad (4.6a)$$

$$\bar{\mathbf{u}}_j^{(\kappa+1)} = \bar{\mathbf{u}}_j^{(*)} + \Delta t \mathbf{s} \left(\bar{\mathbf{u}}_j^{(\kappa+1)} \right). \quad (4.6b)$$

We recapitulate the arguments from e.g. [3, 42] to show that (4.6a) preserves realizability. We have that

$$\begin{aligned} \bar{\mathbf{u}}_j^{(*)} &= \langle \psi_* \rangle \\ \psi_* &= \hat{\psi}_{\bar{\mathbf{u}}_j^{(\kappa)}} - \frac{\Delta t}{\Delta x} \left(\max(\mu, 0) \left(\hat{\psi}_{\bar{\mathbf{u}}_j^{(\kappa)}} - \hat{\psi}_{\bar{\mathbf{u}}_{j+1}^{(\kappa)}} \right) + \min(\mu, 0) \left(\hat{\psi}_{\bar{\mathbf{u}}_{j-1}^{(\kappa)}} - \hat{\psi}_{\bar{\mathbf{u}}_j^{(\kappa)}} \right) \right) \\ &\geq \left(1 - \frac{\Delta t}{\Delta x} \right) \hat{\psi}_{\bar{\mathbf{u}}_j^{(\kappa)}} \stackrel{(4.5)}{\geq} 0, \end{aligned}$$

where $\hat{\psi}_{\bar{\mathbf{u}}_{j-1}^{(\kappa)}}, \hat{\psi}_{\bar{\mathbf{u}}_j^{(\kappa)}}, \hat{\psi}_{\bar{\mathbf{u}}_{j+1}^{(\kappa)}} \geq 0$ are the respective ansätze (2.14) for the moment vectors in cells I_{j-1}, I_j and I_{j+1} . Thus, $\bar{\mathbf{u}}_j^{(*)}$ is generated by the non-negative distribution function ψ_* and is therefore realizable, i.e. $\bar{\mathbf{u}}_j^{(*)} \in \mathcal{R}_{\mathbf{b}}$.

To show a similar result for (4.6b), Corollary 3.5 has to be adopted to the situation. The update has the form

$$\begin{aligned}\bar{\mathbf{u}}_j^{(\kappa+1)} &= \left(\bar{\mathbf{u}}_j^{(*)} + \Delta t \langle \mathbf{b} \bar{Q}_j \rangle \right) + \Delta t \left(\bar{\sigma}_{sj} \mathbf{C} \left(\bar{\mathbf{u}}_j^{(\kappa+1)} \right) - \bar{\sigma}_{aj} \bar{\mathbf{u}}_j^{(\kappa+1)} \right) \\ &= \underbrace{\left\langle \mathbf{b} \left(\hat{\psi}_{\bar{\mathbf{u}}_j^{(*)}} + \Delta t \bar{Q}_j \right) \right\rangle}_{\substack{\geq 0 \\ \in \mathcal{R}_{\mathbf{b}}}} + \Delta t \left(\bar{\sigma}_{sj} \mathbf{C} \left(\bar{\mathbf{u}}_j^{(\kappa+1)} \right) - \bar{\sigma}_{aj} \bar{\mathbf{u}}_j^{(\kappa+1)} \right).\end{aligned}$$

This can be stated equivalently as

$$(1 + \Delta t \bar{\sigma}_{aj}) \bar{\mathbf{u}}_j^{(\kappa+1)} = \left\langle \mathbf{b} \left(\hat{\psi}_{\bar{\mathbf{u}}_j^{(*)}} + \Delta t \bar{Q}_j \right) \right\rangle + \Delta t \bar{\sigma}_{sj} \mathbf{C} \left(\bar{\mathbf{u}}_j^{(\kappa+1)} \right).$$

Since the realizable set is a convex cone and $\bar{\sigma}_{aj} \geq 0$, $(1 + \Delta t \bar{\sigma}_{aj})^{-1} \left\langle \mathbf{b} \left(\hat{\psi}_{\bar{\mathbf{u}}_j^{(*)}} + \Delta t \bar{Q}_j \right) \right\rangle \in \mathcal{R}_{\mathbf{b}}$. Thus,

$$\bar{\mathbf{u}}_j^{(\kappa+1)} = (1 + \Delta t \bar{\sigma}_{aj})^{-1} \left\langle \mathbf{b} \left(\hat{\psi}_{\bar{\mathbf{u}}_j^{(*)}} + \Delta t \bar{Q}_j \right) \right\rangle + (1 + \Delta t \bar{\sigma}_{aj})^{-1} \Delta t \bar{\sigma}_{sj} \mathbf{C} \left(\bar{\mathbf{u}}_j^{(\kappa+1)} \right)$$

is of the form that Corollary 3.5 can be applied (with suitable redefinitions of Δt). Note that boundedness and continuity of the physical parameters are necessary such that a similar modification of Lemma 3.4 is still valid.

Thus $\bar{\mathbf{u}}_j^{(\kappa+1)} \in \mathcal{R}_{\mathbf{b}}$, which completes the proof. \square

Remark 4.2. Using an explicit discretization of the source term, the CFL condition (4.5) has to be modified to

$$\Delta t \leq \frac{1}{\frac{1}{\Delta x} + \max_{j, \kappa} (\bar{\sigma}_{aj}(t_\kappa) + \bar{\sigma}_{sj}(t_\kappa))}$$

to preserve realizability (if possible at all) [3, 42].

5. Numerical experiments

5.1. Manufactured solution

In general, analytical solutions for minimum-entropy models are not known. Therefore, to test the convergence and efficiency of our scheme, the method of manufactured solutions is used, following the target solution given in [42]. The solution is defined on the spatial domain $X = (-\pi, \pi)$ with periodic boundary conditions.

A kinetic density in the form of the entropy ansatz is given by

$$\begin{aligned}\psi_a(t, x, \mu) &= \exp(\alpha_0(t, x) + \alpha_1(t, x)\mu), \\ \alpha_0(t, x) &= -K - \sin(x - t) - b, \\ \alpha_1(t, x) &= K + \sin(x - t).\end{aligned}\tag{5.1}$$

A source term is defined by applying the transport operator to ψ_a , giving

$$Q(t, x, \mu) := \partial_t \psi_a(t, x, \mu) + \mu \partial_x \psi_a(t, x, \mu) + \sigma_a(t, x) \psi_a(t, x, \mu),$$

where

$$\sigma_a(t, x) := 4(1 - \cos(x - t)).$$

Thus, by inserting this Q into (2.1) and setting $\sigma_s = 0$, ψ_a is a solution of (2.1).

A straightforward computation shows that $Q \geq 0$ (for any b and K), which means that Theorem 4.1 can be applied to the resulting moment system.

Furthermore, b is chosen as

$$b = -K + 1 - \log\left(\frac{K - 1}{2 \sinh(K - 1)}\right)$$

so that the maximum value of $\langle \psi_a \rangle$ for $(t, x) \in [0, t_f] \times X$ is one. As K is increased, ψ_a converges to a Dirac delta at $\mu = 1$.

Since ψ_a has the form of an entropy ansatz, $\mathbf{u}_a = \langle \mathbf{b} \psi_a \rangle$ is also a solution of (2.8) whenever 1 and μ are in the linear span of the basis \mathbf{b} . Notice also that \mathbf{u}_a approaches the boundary of realizability as K is increased.

The final time is chosen to be $t_f = \pi/5$ while $K \in \{2, 25\}$ is used, for which the normalized first-order moment satisfies $\frac{u_{a,1}}{u_{a,0}} \in \{[0.313, 0.672], [0.958, 0.962]\}$ (recall that $|u_{a,1}| \leq u_{a,0}$ is necessary for realizability).

In the following, the M_3 model is used so that the results include the effects of the numerical optimization.

Errors are computed in the zeroth moment of the solution $u_{a,0}(t, x) := \langle \psi_a(t, x, \cdot) \rangle$. Then L_1 - and L_∞ -errors for the zeroth moment $u_{h,0}(t, x)$ (that is, the zeroth component of a numerical solution \mathbf{u}_h) are defined as

$$E_h^1 = \Delta x \sum_{j=1}^{n_x} \left| \overline{u_{a,0,j}}(t_f) - \overline{u_{0,j}}(t_f) \right| \quad \text{and} \quad E_h^\infty = \max_{j=1, \dots, n_x} \left| \overline{u_{a,0,j}}(t_f) - \overline{u_{0,j}}(t_f) \right|, \quad (5.2)$$

respectively. The observed convergence order ν is defined by

$$\frac{E_{h_1}^p}{E_{h_2}^p} = \left(\frac{\Delta x_1}{\Delta x_2} \right)^\nu, \quad (5.3)$$

where $E_{h_i}^p$, $i \in \{1, 2\}$, $p \in \{1, \infty\}$, is the L_p -error E_h^p for the numerical solution using cell size Δx_i .

A convergence table for two different values of K is presented in Table 1. They correspond in spatial average to the sets of normalized moments $\phi = (0.515, 0.463, 0.333)^T$ ($K = 2$) and $\phi = (0.960, 0.923, 0.889)^T$ ($K = 25$) with relative distance to the realizability boundary (absolute distance divided by the maximal possible distance) of 5.016% and 0.0006%, respectively.

n_x	$K = 2$				$K = 25$			
	E_h^1	ν	E_h^∞	ν	E_h^1	ν	E_h^∞	ν
40	5.332e-02	—	2.355e-02	—	7.063e-03	—	2.633e-03	—
80	2.713e-02	0.97	1.208e-02	0.96	3.558e-03	0.99	1.329e-03	0.99
160	1.368e-02	0.99	6.118e-03	0.98	1.792e-03	0.99	6.671e-04	0.99
320	6.862e-03	1.00	3.078e-03	0.99	9.035e-04	0.99	3.341e-04	1.00
640	3.444e-03	0.99	1.554e-03	0.99	4.655e-04	0.96	1.684e-04	0.99

Table 1: L_1 - and L_∞ -errors and observed convergence order ν for the IMEX kinetic scheme with M_3 manufactured solution (5.1) and optimization gradient tolerance $\tau = 10^{-6}$.

It can be observed that the expected convergence rates are achieved both in L_1 - and L_∞ -errors.

Remark 5.1. *The scheme is not convergent for arbitrarily large values of K . For big K , the numerical solution veers so close to the boundary of the realizable set that the optimization has to use regularization, thus introducing errors into the solution. This has been shown in [3] for a simpler convergence test and was also observed before in [1].*

5.2. Plane source

In this test case an isotropic distribution with all mass concentrated in the middle of an infinite domain $x \in (-\infty, \infty)$ is defined as initial condition, i.e.

$$\psi_{t=0}(x, \mu) = \psi_{\text{vac}} + \delta(x),$$

where the small parameter $\psi_{\text{vac}} = 0.5 \times 10^{-8}$ is used to approximate a vacuum. In practice, a bounded domain must be used which is large enough that the boundary should have only negligible effects on the solution. For the final time $t_f = 1$, the domain is set to $X = [-1.2, 1.2]$ (recall that for all presented models the maximal speed of propagation is bounded in absolute value by one [3, 28]).

At the boundary the vacuum approximation

$$\psi_b(t, x_L, \mu) \equiv \psi_{\text{vac}} \quad \text{and} \quad \psi_b(t, x_R, \mu) \equiv \psi_{\text{vac}}$$

is used again. Furthermore, the physical coefficients are set to $\sigma_s \equiv 1$, $\sigma_a \equiv 0$ and $Q \equiv 0$.

All solutions are computed with an even number of cells, so the initial Dirac delta lies on a cell boundary. Therefore it is approximated by splitting it into the cells immediately to the left and right. In Figure 3, only positive x are shown since the solutions are always symmetric around $x = 0$.

For an intense discussion of the solution of the moment models see e.g. [40, 41]. For convenience, the space-time behaviour of the density ρ for M_1 to M_3 are shown in Figure 2.

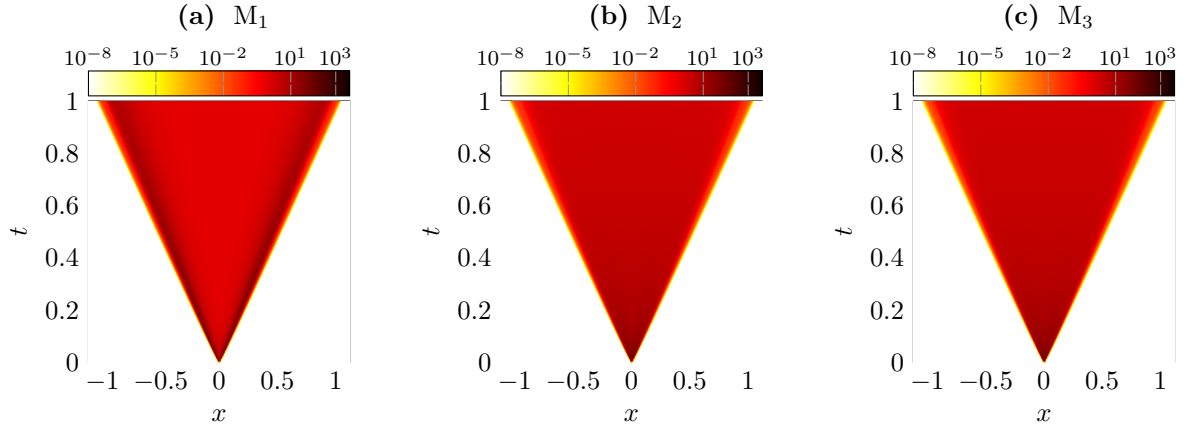


Figure 2: Results for the plane-source test in the space-time domain in a logarithmic scale.

A known problem of the minimum-entropy approach is the fact that close to the realizability boundary the moment system becomes ill-conditioned [2]. We investigate the relative distance of the plane-source M_N solutions to the boundary of the *normalized realizable set*

$$\mathcal{R}_{\mathbf{b}}|_{u_0=1} = \{\mathbf{u} : \exists \psi(\Omega) \geq 0, u_0 = \langle \psi \rangle = 1, \text{ such that } \mathbf{u} = \langle \mathbf{b}\psi \rangle\}$$

as the ratio of the euclidean distance to the realizability boundary and the maximal possible distance, i.e.

$$d_r(\mathbf{u}, \partial\mathcal{R}_{\mathbf{b}}|_{u_0=1}) = \frac{d(\mathbf{u}, \partial\mathcal{R}_{\mathbf{b}}|_{u_0=1})}{\max_{\hat{\mathbf{u}} \in \mathcal{R}_{\mathbf{b}}|_{u_0=1}} d(\hat{\mathbf{u}}, \partial\mathcal{R}_{\mathbf{b}}|_{u_0=1})}, \quad d(\mathbf{u}, \partial\mathcal{R}_{\mathbf{b}}|_{u_0=1}) = \min_{\hat{\mathbf{u}} \in \partial\mathcal{R}_{\mathbf{b}}|_{u_0=1}} \|\mathbf{u} - \hat{\mathbf{u}}\|_2.$$

The maximal distances are

$$\begin{aligned} \max_{\hat{\mathbf{u}} \in \mathcal{R}_{\mathbf{b}}|_{u_0=1}} d(\hat{\mathbf{u}}, \partial\mathcal{R}_{\mathbf{b}}|_{u_0=1}) &= 1 && \text{for } M_1, \\ \max_{\hat{\mathbf{u}} \in \mathcal{R}_{\mathbf{b}}|_{u_0=1}} d(\hat{\mathbf{u}}, \partial\mathcal{R}_{\mathbf{b}}|_{u_0=1}) &= \frac{1}{2} && \text{for } M_2, \text{ and} \\ \max_{\hat{\mathbf{u}} \in \mathcal{R}_{\mathbf{b}}|_{u_0=1}} d(\hat{\mathbf{u}}, \partial\mathcal{R}_{\mathbf{b}}|_{u_0=1}) &= \frac{1}{5} && \text{for } M_3. \end{aligned}$$

The results are shown in Figure 3.

While the relative distance in case of the M_1 model (Figures 3a and 3b) is directly related the normalized first moment ϕ_1 by $d_r(\mathbf{u}, \partial\mathcal{R}_{\mathbf{b}}|_{u_0=1}) = 1 - |\phi_1|$ (resulting in small distances only close to the peak at $t = \pm x$), the distances in case of the higher-order models become smaller even in the interior of the set $\{|x| \leq t\}$. The minimal values that occurred are 0.0039 (M_1), $2.2147 \cdot 10^{-5}$ (M_2) and $9.0981 \cdot 10^{-7}$ (M_3), showing that the underlying moment problem becomes harder to solve with increasing moment order N .

Figures 3d and 3f show a histogram (300 · 300 bins) of the M_2 and M_3 solution in the $\phi_1 - \phi_N$ phase space (where N is either 2 or 3, respectively). The histogram is built out of the solution values at the 10000 cell centres and 100 time frames. The boundary of the (projected) normalized realizable set is depicted as a black, dashed line. In case of the M_2 model, it is visible that mostly the lower part of the realizable set is filled with particles, complemented with a stream of particles connected to the isotropic point $\phi_{\text{iso}} = (0, \frac{1}{3})$. No particles occur close to the point of maximal distance $\phi = (0, \frac{1}{2})$. Thus, the relative distance for M_2 is always strictly smaller than 1. A similar effect occurs in case of the M_3 model, but less pronounced.

6. Conclusions and outlook

We derived an implicit-explicit scheme for moment systems that are generated by a non-negative ansatz. This scheme preserves realizability under a standard CFL condition, even in the case of stiff source terms (e.g. strong scattering or absorption), while the implicit systems have to be solved only locally in every space-time cell. In many cases, these implicit systems are linear, resulting in a very efficient algorithm.

Convergence of the algorithm was tested against a manufactured solution, showing the designed first order. Furthermore, the plane-source problem served as benchmark test, showing how close to the realizability boundary the scheme can get.

While this first-order scheme is easy to implement, the benefit of high-order schemes in terms of efficiency is necessary to obtain reasonable approximations in higher dimensions in an appropriate time. Future work will investigate how to couple higher-order IMEX schemes with the fully-explicit, high-order kinetic [42] and discontinuous-Galerkin scheme [3], removing the stiffness from these two methods.

Furthermore, it is unclear if the mixed-moment model [14, 41] in combination with the Laplace-Beltrami operator Δ_μ fulfils the assumptions of Theorem 4.1 (it contains the microscopic quantity $\hat{\psi}_{\mathbf{u}}(0)$, i.e. the solution of (3.3) depends on the chosen ansatz). Nevertheless, (4.1) performs well in practice even in this situation, which could mean that either the above assumptions are fulfilled or Theorem 4.1 can be extended to a weaker set of assumptions.

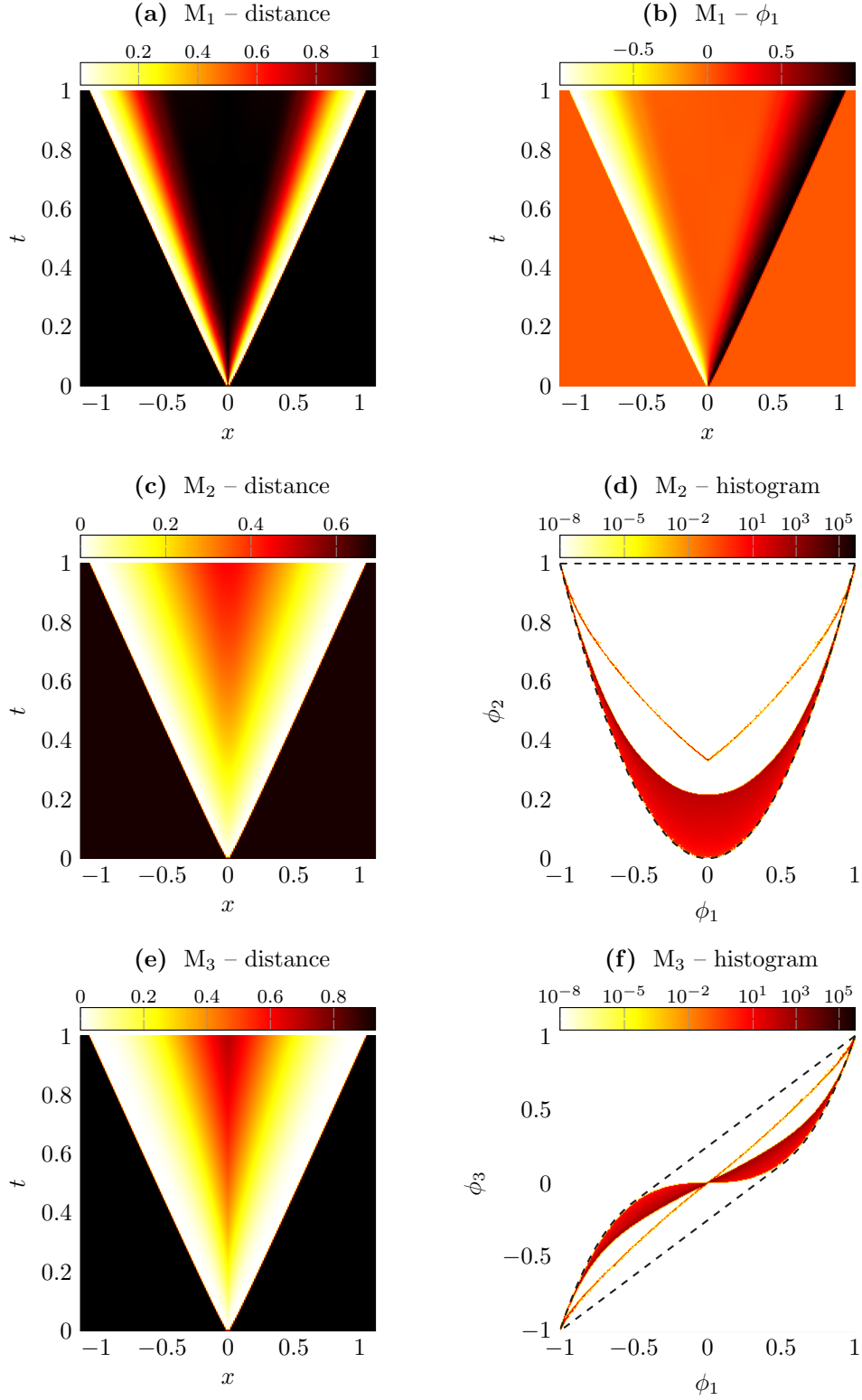


Figure 3: Relative distance to the realizability boundary and related quantities for the plane-source test.

References

- [1] G. W. ALLDREDGE, C. D. HAUCK, D. P. O'LEARY, AND A. L. TITS, *Adaptive change of basis in entropy-based moment closures for linear kinetic equations*, Journal of Computational Physics, 258 (2014), pp. 489–508.
- [2] G. W. ALLDREDGE, C. D. HAUCK, AND A. L. TITS, *High-Order Entropy-Based Closures for Linear Transport in Slab Geometry II: A Computational Study of the Optimization Problem*, SIAM Journal on Scientific Computing, 34 (2012), pp. B361–B391.
- [3] G. W. ALLDREDGE AND F. SCHNEIDER, *A realizability-preserving discontinuous Galerkin scheme for entropy-based moment closures for linear kinetic equations in one space dimension*, Journal of Computational Physics, 295 (2015), pp. 665–684.
- [4] U. ASCHER, S. RUUTH, AND R. SPITERI, *Implicit-explicit Runge-Kutta methods for time-dependent partial differential equations*, Applied Numerical Mathematics, (1997).
- [5] T. A. BRUNNER, *Forms of approximate radiation transport*, SAND2002-1778, Sandia National Laboratory, (2002).
- [6] R. E. CURTO AND L. A. FIALKOW, *Solution of the Truncated Complex Moment Problem for Flat Data*, 1996.
- [7] R. E. R. CURTO AND L. A. FIALKOW, *Recursiveness, positivity, and truncated moment problems*, Houston J. Math, 17 (1991), pp. 603–636.
- [8] P. DEGOND AND S. MAS-GALLIC, *Existence of solutions and diffusion approximation for a model Fokker-Planck equation*, Transport Theory and Statistical Physics, 16 (1987), pp. 37–41.
- [9] B. DUBROCA AND J.-L. FEUGEAS, *Entropic Moment Closure Hierarchy for the Radiative Transfer Equation*, C. R. Acad. Sci. Paris Ser. I, 329 (1999), pp. 915–920.
- [10] B. DUBROCA, M. FRANK, A. KLAR, AND G. THÖMMES, *Half space moment approximation to the radiative heat transfer equations*, ZAMM, 83 (2003), pp. 853–858.
- [11] B. DUBROCA AND A. KLAR, *Half-moment closure for radiative transfer equations*, Journal of Computational Physics, 180 (2002), pp. 584–596.
- [12] R. FOX, *A quadrature-based third-order moment method for dilute gas-particle flows*, Journal of Computational Physics, 227 (2008), pp. 6313–6350.
- [13] ———, *Higher-order quadrature-based moment methods for kinetic equations*, Journal of Computational Physics, 228 (2009), pp. 7771–7791.
- [14] M. FRANK, H. HENSEL, AND A. KLAR, *A fast and accurate moment method for the Fokker-Planck equation and applications to electron radiotherapy*, SIAM Journal on Applied Mathematics, 67 (2007), pp. 582–603.
- [15] C. K. GARRETT AND C. D. HAUCK, *A Comparison of Moment Closures for Linear Kinetic Transport Equations: The Line Source Benchmark*, Transport Theory and Statistical Physics, (2013).
- [16] E. M. GELBARD, *Simplified spherical harmonics equations and their use in shielding problems*, Tech. Report WAPD-T-1182, Bettis Atomic Power Laboratory, 1961.
- [17] W. HACKENBROCH AND A. THALMAIER, *Stochastische Analysis: eine Einführung in die Theorie der stetigen Semimartingale*, Mathematische Leitfäden, B.G. Teubner, 1994.
- [18] C. D. HAUCK, *High-order entropy-based closures for linear transport in slab geometry*, Commun. Math. Sci. v9, (2010).
- [19] H. HENSEL, R. IZA-TERAN, AND N. SIEDOW, *Deterministic model for dose calculation in photon radiotherapy*, to appear in Phys. Med. Biol.
- [20] E. P. HSU, *Stochastic Analysis on Manifolds*, Contemporary Mathematics, American Mathematical Soc., 2002.
- [21] M. JUNK, *Maximum entropy for reduced moment problems*, Math. Meth. Mod. Appl. Sci., 10 (2000), pp. 1001–1025.
- [22] D. S. KERSHAW, *Flux Limiting Nature's Own Way: A New Method for Numerical Solution of the Transport Equation*, (1976).
- [23] H.-H. KUO, *Introduction to Stochastic Integration*, Springer, 2006.
- [24] C. LAM AND C. P. GROTH, *Numerical Prediction of Three-Dimensional Non-Equilibrium Flows Using the Regularized Gaussian Moment Closure*, in 52nd Aerospace Sciences Meeting, AIAA SciTech, American Institute of Aeronautics and Astronautics, jan 2014.
- [25] E. W. LARSEN AND G. C. POMRANING, *The PN Theory as an Asymptotic Limit of Transport Theory in Planar Geometry I: Analysis*, Nuclear Science and Engineering, 109 (1991), pp. 49–75.
- [26] C. D. LEVERMORE, *Moment closure hierarchies for kinetic theories*, Journal of Statistical Physics, 83 (1996), pp. 1021–1065.
- [27] ———, *Moment closure hierarchies for the Boltzmann-Poisson Equation*, Journal of Statistical Physics, 83 (1996), pp. 1021–1065.
- [28] ———, *Moment Closure Hierarchies for the Boltzmann-Poisson Equation*, VLSI Design, 6 (1998), pp. 97–101.
- [29] ———, *Boundary conditions for moment closures*, Institute for Pure and Applied Mathematics University of California, Los Angeles, CA on May, 27 (2009).
- [30] E. E. LEWIS AND J. W. F. MILLER, *Computational Methods in Neutron Transport*, John Wiley and Sons, New York, 1984.
- [31] J. G. McDONALD AND C. P. T. GROTH, *Towards realizable hyperbolic moment closures for viscous heat-conducting gas flows based on a maximum-entropy distribution*, Continuum Mechanics and Thermodynamics, 25 (2012), pp. 573–603.
- [32] E. OLBRANT, C. D. HAUCK, AND M. FRANK, *A realizability-preserving discontinuous Galerkin method for the M1 model of radiative transfer*, Journal of Computational Physics, 231 (2012), pp. 5612–5639.
- [33] G. C. POMRANING, *Variational boundary conditions for the spherical harmonics approximation to the neutron transport equation*, Annals of Physics, 27 (1964), pp. 193–215.
- [34] ———, *The Fokker-Planck operator as an asymptotic limit*, Math. Mod. Meth. Appl. Sci., 2 (1992), pp. 21–36.
- [35] H. RISKEN, *The Fokker-Planck Equation: Methods of Solution and Applications*, Lecture Notes in Mathematics, Springer Berlin Heidelberg, 1996.

- [36] J. RITTER, A. KLAR, AND F. SCHNEIDER, *Partial-moment minimum-entropy models for kinetic chemotaxis equations in one and two dimensions*, (2016).
- [37] R. P. RULKO, E. W. LARSEN, AND G. C. POMRANING, *The PN Theory as an Asymptotic Limit of Transport Theory in Planar Geometry II: Numerical Results*, Nuclear Science and Engineering, 109 (1991), pp. 76–85.
- [38] F. SCHNEIDER, *Kershaw closures for linear transport equations in slab geometry I: Model derivation*, Journal of Computational Physics, 322 (2016), pp. 905–919.
- [39] ———, *Kershaw closures for linear transport equations in slab geometry II: high-order realizability-preserving discontinuous-Galerkin schemes*, Journal of Computational Physics, 322 (2016), pp. 920–935.
- [40] ———, *Moment models in radiation transport equations*, Dr. Hut Verlag, 2016.
- [41] F. SCHNEIDER, G. W. ALLDREDGE, M. FRANK, AND A. KLAR, *Higher Order Mixed-Moment Approximations for the Fokker–Planck Equation in One Space Dimension*, SIAM Journal on Applied Mathematics, 74 (2014), pp. 1087–1114.
- [42] F. SCHNEIDER, G. W. ALLDREDGE, AND J. KALL, *A realizability-preserving high-order kinetic scheme using WENO reconstruction for entropy-based moment closures of linear kinetic equations in slab geometry*, Kinetic and Related Models, (2015).
- [43] F. SCHNEIDER, J. KALL, AND A. ROTH, *First-order quarter- and mixed-moment realizability theory and Kershaw closures for a Fokker–Planck equation in two space dimensions*, (2015).
- [44] H. STRUCHTRUP, *Kinetic schemes and boundary conditions for moment equations*, Zeitschrift für angewandte Mathematik und Physik, 51 (2000), p. 346.
- [45] V. VIKAS, C. D. HAUCK, Z. J. WANG, AND R. O. FOX, *Radiation transport modeling using extended quadrature method of moments*, Journal of Computational Physics, 246 (2013), pp. 221–241.
- [46] C. YUAN, F. LAURENT, AND R. FOX, *An extended quadrature method of moments for population balance equations*, Journal of Aerosol Science, 51 (2012), pp. 1–23.
- [47] X. ZHANG AND C. W. SHU, *On positivity-preserving high order discontinuous Galerkin schemes for compressible Euler equations on rectangular meshes*, Journal of Computational Physics, 229 (2010), pp. 8918–8934.
- [48] X. ZHANG, Y. XIA, AND C.-W. SHU, *Maximum-Principle-Satisfying and Positivity-Preserving High Order Discontinuous Galerkin Schemes for Conservation Laws on Triangular Meshes*, Journal of Scientific Computing, (2011), pp. 1–34.